

WindSat Polarimetric View of Greenland

¹Li Li, ¹Peter Gaiser and ¹Elizabeth Twarog

¹Remote Sensing Division
Naval Research Laboratory
Washington, DC 20375, USA
E-mail: li.li@nrl.navy.mil

²David G. Long and ³Mary Albert

²Center for Remote Sensing, Brigham Young University
Provo, Utah 84602, USA
³Cold Regions Research and Engineering Laboratory
Hanover, New Hampshire 03755, USA

Abstract— WindSat has systemically collected the first global passive polarimetric data over both land and ocean at three frequencies: 10.7, 18.7 and 37 GHz, including the brightness temperatures at vertical and horizontal polarizations, and the real and imaginary parts of the cross-correlation of the vertical and horizontal polarizations. Prior to the launch of WindSat, it was commonly believed that land polarimetric signatures at satellite footprint scales are below instrumental noise levels and do not have any useful geophysical information. On the contrary, WindSat polarimetric data exhibit distinct geophysical and observation geometry signatures, particularly over Greenland and Antarctic where the signatures are related to snow accumulation, melting and metamorphism. The third and fourth Stokes parameters show well defined, large azimuth modulation which is correlated with geophysical variations, particularly with snow metamorphism, and has consistent seasonal variation. We use simple empirical models to separate and quantify such azimuthal modulations and geophysical changes. By comparing the temporal variations of harmonic coefficients and brightness temperature signatures in vertical and horizontal polarization channels, we find that both volume and surface scattering have important contributions to the polarimetric signature. Such signatures are relatively weak in the summer, when sastrugi are small and surface scattering is significant, and are strongest in spring, when the sastrugi are larger and volume scattering is important.

Keywords—polarimetric microwavr radiometry; WindSat; snow; Greenland

I. INTRODUCTION

WindSat, launched in January 2003 and currently in operation, is the first spaceborne microwave polarimetric radiometer to measure all four elements of Stokes vector, namely the brightness temperatures at vertical and horizontal polarizations, and the real and imaginary parts of the cross-correlation of the vertical and horizontal polarizations [1]. WindSat was designed to measure ocean surface wind speeds as well as wind directions by including the third and fourth Stokes parameters, which are mostly related to the asymmetric structures of the ocean surface roughness. Prior to the launch of WindSat, it was a commonly believed that land polarimetric signatures at satellite footprint scales would be below the instrument noise level and would not carry any useful geophysical information. However, on the contrary, post-launch data processing reveals significant land signals in the third and fourth Stokes channels, particularly over Greenland and the Antarctic ice sheets. For example, Fig. 1 depicts the third and fourth Stokes measurements at 10.7 GHz over the North Hemisphere for the period of 2/1-9/2004. Although the

third Stokes shows the most coherent large scale signals over the ocean, and it also shows a significant 0.5 to 1 K signal over land. Over Greenland the third Stokes parameter varies between ± 10 K while the fourth Stokes parameter varies between -10 and +20 K, which is up to ten times larger than those observed over the ocean. In this paper, we focus our analysis on WindSat over Greenland, charactering its polarimetric signatures and its associated temporal and spatial variations.

As the second largest ice sheet in the world, the Greenland icesheet is the most environmentally sensitive Earth media, playing a significant role in global sea level and climate changes. Understanding this polarimetric signature, uniquely afforded by WindSat, and its relation with the snow properties and microstructures could have a profound impact on climate study.

II. WINDSAT DATA ANALYSIS

A. Methodology

The objective of this study is to define the passive microwave signature of Greenland from WindSat data. By observing the changes in the microwave signature, one can infer the temporal and spatial variations in the physical properties of the ice sheet. A simple and effective way to define the microwave signature is to construct empirical observation model that can describe and separate different effects in the measurements and summarize the microwave signature in a small number of model parameters. Over Greenland, the vertical and horizontal polarized brightness temperatures respond mostly to the grain size, density and temperature of the snow, ice and firn; while the third and fourth Stokes parameters respond most strongly to the asymmetric structure of the snow-pack, and can be strong functions of the observation geometry, including the azimuth look angle. Therefore it is essential to consider the azimuth modulations of the third and fourth Stokes parameters and separate observation geometry effects from environmental variations. Since vertical and horizontal brightness temperatures have been well investigated in other studies in the past, here we focus on modeling of polarimetric signatures in the third and fourth Stokes parameters

Given the constant Earth incidence angle of WindSat conical scanning geometry, the 3rd Stokes (U) and 4th Stokes (V) brightness temperatures over Greenland are functions of satellite azimuth look angle (observation geometry) and ice-sheet characteristics [2][3]. We thus adopt a simple empirical model for the polarimetric emissions,

This research is supported in part by the NRL Ocean and Atmospheric Science and Technology Program and the NPOESS Integrated Program Office.)

$$\begin{bmatrix} U \\ V \end{bmatrix} = \begin{bmatrix} U_0 + U_1 \sin(\varphi - \phi_1) + U_2 \sin 2(\varphi - \phi_2) \\ V_0 + V_1 \sin(\varphi - \phi_1) + V_2 \sin 2(\varphi - \phi_2) \end{bmatrix}$$

where φ is observation azimuth angle; $\{U_i\}$ and $\{V_i\}$ are the coefficient of the azimuth modulation, and $\{\Phi_i\}$ and $\{\phi_i\}$ are the orientations of different harmonics. In the following, our goal is to fit such an equation to time series of WindSat observations for a particular location. Temporal and spatial variations of these coefficients can provide insight about the microwave scattering mechanism and its related geophysical processes.

B. Data Preparation and Azimuth Modulation Analysis

The seasonal variations of the Stokes parameters at locations in different snow zones in Greenland reflect the transitions in surface and subsurface properties. Our focus is on the time-series analysis of the third and fourth Stokes parameters, since the first two Stokes parameters (vertically and horizontally polarized brightness temperatures) are mostly dominated by the snow dielectric properties and physical temperatures, not observation geometry, we compare the time-series of the third and fourth Stokes parameter harmonic coefficients to the vertically and horizontally polarized brightness temperatures to provide physical insights into the cause of variations in the third and fourth Stokes parameters.

The third and fourth Stokes parameters are very sensitive to asymmetric structures of snow media and therefore the sensor observation geometry and are less sensitive to physical temperatures of snow. As a result, the third and fourth Stokes parameters have well defined dependencies on sensor azimuth looking angle when compared with dual-polarized radiometer data and scatterometer data [2], where it has always been a challenging task to separate diurnal effects from azimuth modulations. For WindSat data, the 3rd and 4th Stokes channel data exhibits little diurnal effects throughout the year and fit well to the empirical model. Fig. 2 illustrates the azimuthal variation of WindSat polarimetric data extracted from the Summit site for April 2003. All six WindSat polarimetric channels are shown here. The measurements centered on 210° and 340° compass azimuth angle correspond to satellite descending and ascending passes, respectively. The solid line is the fitted second-order harmonic model. The left column shows the third Stokes parameter while the right column shows the fourth Stokes parameter. The top row is 10.7 GHz, the center row is 18.7 GHz and the bottom row is 37 GHz. Clearly, there are well-pronounced azimuth dependences on all the channels. The WindSat data fits to the empirical model are excellent, as depicted by the solid lines. We also fitted the model to WindSat data from different months and obtained similar results, which suggest that WindSat polarimetric data can be modeled well using the second order harmonic model.

III. RESULTS

A. Dry-Snow Zone

In the Greenland dry-snow region, the top layer is light-snow with annual accumulation of about 30 cm snow-water-equivalent per year, the typical snow density is 0.3 g/cm^3 and

the mean grain diameters are about 0.23 mm. The firn beneath the top snow layer has a typical density of 0.4 g/cm^3 [4]. The snow pack can be characterized by Rayleigh spectrum of the reflectivity [5][6], the volume scattering is insignificant at 10.7 GHz but increases quickly for 18.7 and 37 GHz. Again, we extracted EASE-grid data between January and December 2004 from the Summit at (72.5° N , 39.0° W). Fig. 3 shows time-series of WindSat data at 10.7, 18.7 and 37 GHz channels extracted over Summit region.

Fig. 3(a) (top left panel) plots temporal variation of vertical polarization brightness temperature. The 10.7 GHz (black curve) channel has an evident, but small and slow, seasonal variation; while the 18.7 (purple) and 37 GHz (blue) channels show large to very large seasonal brightness temperature variations relative to the 10.7 GHz channel, recall that vertical polarization is sensitive to the physical temperature and properties of the snow-pack. The seasonal increase in snow-pack physical temperature results in higher dielectric loss or microwave absorption, which contributes directly to the increase of brightness temperature in the summer and decrease during the fall. Such seasonal variations peak at different time for the different frequencies. For example, the 10.7 GHz data peaks around early September (Day 240 and 600) while 37 GHz peaks around middle July (Day 190 and 550). Such a phase difference between the two peaks is due to the different penetration depths at 10.7 and 37 GHz. In summer there is a temperature gradient in the snow due to the warming of near-surface layers while the deeper layers are still cold from the previous winter. In addition, the brightness temperature difference of the 18.7 and 37 GHz channels relative to the 10.7 GHz channel demonstrate that seasonal variations that are most intense around middle-winter in late February or early March due to snow temperature changes as well as the volume scattering in the top snow layers. The difference is defined as the Scattering Index (SI) to effectively quantify the volume scattering intensity [7], but it also contains sensitivity differences of snow emissivity at these frequencies. The maximum SI is about 12 K and 23 K at the 18.7 and 37 GHz channels, respectively.

During summer months of July to September, the reduced penetration depth due to higher snow temperatures should decrease the volume scattering and increase the surface scattering depending on layered snow structures. For example, the 18.7 GHz brightness temperature is slightly higher than the 10.7 GHz TB but about 8 K higher than the 37 GHz TB. In this case, the volume scattering is relative weak with low SI values. On the other hand, the summer formation of very small amounts of moisture in the snow associated with warming is sufficient to reduce scattering albedo dramatically, resulting in low polarization difference signatures which is defined as the difference between vertical and horizontal polarization channels [6]. This is illustrated well by the time-series of polarization difference in Fig. 3(b). The polarization difference reaches minimum in July – September (month 7-9 and 19-21 in Fig. 3(b)). We note that while the maximum air temperature in the summer reaches only as high as -4° C , for air temperature above -10° C , the vapor pressure of the ice increases, leading to increased vapor transport and the formation of a thin liquid surface layer on individual snow crystals. This small amount of

liquid water can significantly alter the dielectric constant of the snow and accelerates diagenetic changes in the snow structure. Therefore the observed WindSat wet snow signatures are consistent with Summit temperature climatology. Ashcraft and Long [3][8] also found similar summer wetness signatures using the radiometer (SSM/I) and scatterometer (NSCAT) data at the Summit and in the dry-snow zone.

In Fig. 3(c) to (f), the time-series of first and second order harmonic coefficients are depicted for the third and fourth Stokes parameters at 10.7, 18.7 and 37 GHz channels at the Summit study site. The first harmonic coefficients $\{U1\}$ and $\{V1\}$ describe the scattering signatures that are related to the asymmetric structure of the snow-pack, possibly induced by the surface slope or skewness of snow sastrugi. The second harmonic coefficients $\{U2\}$ and $\{V2\}$ describe asymmetric features of the snow-pack in the directions parallel and orthogonal to the sastrugi direction. Overall, all the harmonic coefficients can reach as high as 10 K, which are very significant when compared with the 2 to 3 K maximum azimuth variation observed over ocean, where volume scattering is negligible. The 10.7 GHz third Stokes and 37 GHz fourth Stokes seem to be the most sensitive channels to snow-pack variations and have strongest seasonal signals. For all three frequencies, the fourth Stokes signals are about the same strength as the third Stokes over Greenland, which is a striking contrast to a relatively weak fourth Stokes generated by ocean surface scattering at the same frequencies, indicating that volume scattering contributed significantly to the polarimetric signals. All harmonic coefficients peak around later winter to early spring when the sastrugi are largest [9], and are weak in the middle summer when the sastrugi are smallest.

B. Wet-Snow Zone

To examine melting signatures, we extracted a time-series of WindSat data at the well studied ETH/CU camp site (69.6°N, 49.3°W) in the wet-snow zone, as shown in Fig. 4. This site was used by [10] to develop SSM/I snowmelt algorithm for Greenland. In the summer, significant melt occurs around the morning ascending passes, creating the polarimetric signatures of wet-snow that are very different from dry-snow. When there is significant snow wetness, the scattering albedo is dramatically reduced to very small value, and the large change in dielectric properties limits the penetration depth to a few wavelengths beneath the surface. Therefore the surface scattering dominates volume scattering for wet-snow. With the near absence of volume scattering in the snow medium, the snow-pack becomes a nearly blackbody radiator, which is illustrated by the high summer response in Fig. 4(a). From June to September (day 150 to 250), the brightness temperatures of all frequencies approaches the physical temperature (273 K) and is essentially frequency independent, a feature of strong snow melting signature. For the descending passes which occur during the night, refreezing of the wet or saturated snow-pack generated very large snow grains and much deeper penetration. As a result, the scattering mechanism switches from surface scattering dominated in day to volume scattering dominated during the night. For example, the scattering index at 37 GHz is less than 10K for the ascending passes and less than 70 K for the descending passes.

It is interesting to note that, outside of summer, the 37 GHz channel is mostly higher than the 18.7 GHz channel when there is no snow melt. Such an increase of brightness temperature with increasing frequency does not suggest an absence of volume scattering in the snow-pack. Grody and Basist [7] found a similar feature in the SSM/I data. They attributed such a feature to the subsurface ice layer generated by summer melting. Thus, surface scattering at this site tends to dominate volume scattering throughout the year except during the nightly refreezing in the summer. Once again, the temporal variations of the third and fourth Stokes parameters are significant and exhibit well defined seasonal variations. Polarimetric signatures are very weak in the summer melt months and are the strongest in the spring months. Although volume scattering is the strongest during the summer refreezing, such a very strong volume scattering does not produce a very strong polarimetric signature. Therefore the polarimetric signals don't have a simple relationship to surface or volume scattering alone, but are affected by their combination and snow-pack structures.

IV. CONCLUSIONS

WindSat polarimetric data exhibit distinct geophysical and observation geometry signatures over Greenland, which are correlated with geophysical variations, including snow microstructure, melting and metamorphism. The third and fourth Stokes parameters have well defined large azimuth modulations and consistent seasonal variations. A second-order empirical model separates and quantifies the azimuth modulation and geophysical change. Such signatures are relatively weak in the summer when surface scattering is significant and sastrugi are small, and strongest in spring when the sastrugi are larger and volume scattering is important. Therefore WindSat provides an unprecedented and unique dataset for environmental and climate studies in the polar region. Furthermore, these results demonstrate that future polarimetric microwave radiometer missions can be exploited for climate studies.

REFERENCES

- [1] Gaiser, P.W., K.M. St. Germain, E.M. Twarog, G.A. Poe, W. Purdy, D. Richardson, W. Grossman, W.L. Jones, D. Spencer, G. Golba, J. Cleveland, L. Choy, R.M. Bevilacqua, and P. Chang, "The WindSat spaceborne polarimetric microwave radiometer: Sensor description and early orbit performance," *IEEE Trans. Geosci. Rem. Sens.*, vol. 42, pp. 2347-2361, 2004.
- [2] Ashcraft, I.S., and D. Long, "Observation and characterization of radar backscatter over Greenland," *IEEE Trans. Geosci. Remote Sensing*, Vol. 43, pp. 225-237, 2005.
- [3] Ashcraft, I.S., and D. Long, "Comparison of Methods for melt detection over Greenland using active and passive microwave measurements," to appear, *Int. J. Remote Sens.*, 2006.
- [4] Long, D.G., and M.R. Drinkwater, "Greenland Ice-sheet Surface Properties Observed by the Seasat-A Scatterometer at Enhanced Resolution," *Journal of Glaciology*, Vol. 40, No. 135, pp. 213-230, 1994.
- [5] Matzler, C. "Passive microwave signatures of landscapes in winter," *Meteorol. Atmos. Phys.*, Vol. 54, pp. 241-260, 1994.
- [6] Ulaby, F., R. Moore, and A.K. Fung, *Microwave remote sensing: active and passive*, volume 3, Massachusetts: Artech House, Inc., 1990.

- [7] Grody, N.C., and A.N. Basist, "Interpretation of SSM/I measurements over Greenland," IEEE Trans. Geosci. Rem. Sens., vol. 35, pp. 360-366, 1997.
- [8] Ashcraft, I.S., and D. Long, "Differentiation between melt and freeze stages of the melt cycle using SSM/I channel ratios," to appear, IEEE Trans. Geosci. Rem. Sens., 2006b.

- [9] Albert, M.R., and R. Hawley, "Seasonal Changes in Snow Surface Roughness Characteristics at Summit, Greenland: Implications for Snow-Air Transfer Processes," Annals of Glaciology, Vol. 35, p. 52-56, 2002.
- [10] Abdalati, W., and K. Steffen, "Snowmelt on the Greenland ice sheet as derived from passive microwave satellite data," J. of Climate, vol. 10, pp. 165-175, 1997.

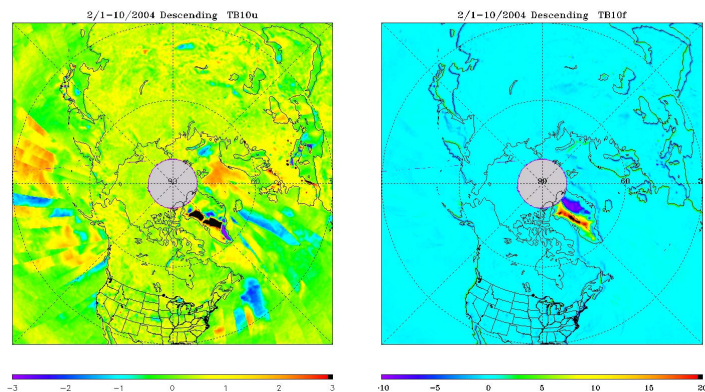


Figure 1. Composite WindSat polarimetric measurements at 10.7 GHz for the third Stokes and fourth Stokes parameters.

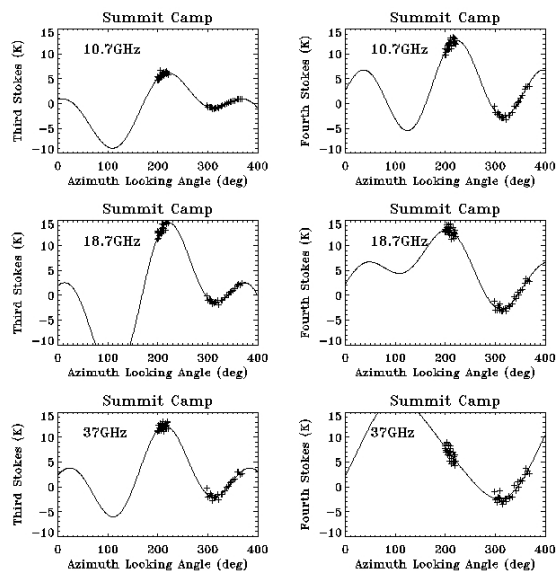


Figure 2. Azimuth modulation of the third and fourth Stokes parameters over the Summit of Greenland during April 2003.

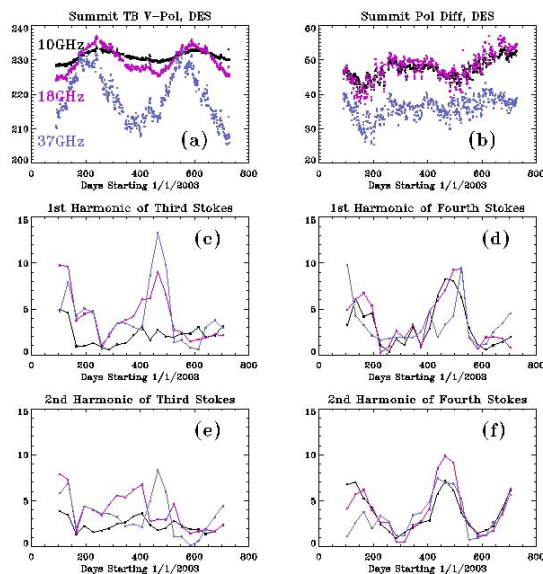


Figure 3. Time series of WindSat observations over the Greenland Summit study site.

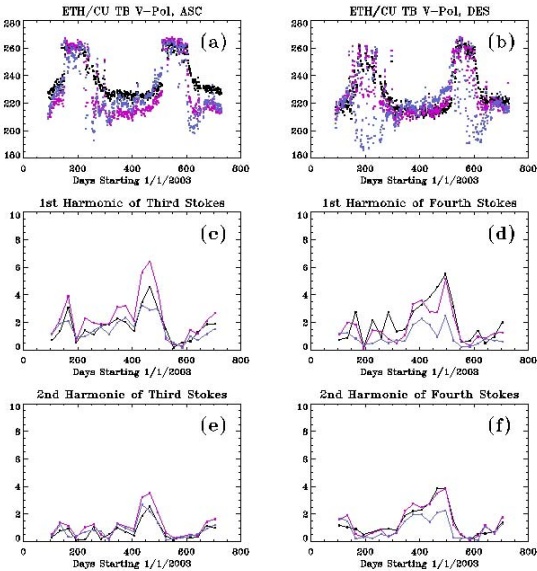


Figure 4. Time series of WindSat observations over the Greenland ETH/CU camp study site.